IEEE Photonics Journal
An IEEE Photonics Society Publication

Open Access

Orthogonal Full-Field Optical Sampling

Volume 11, Number 2, April 2019

Janosch Meier
Arijit Misra
Stefan Preußler
Thomas Schneider

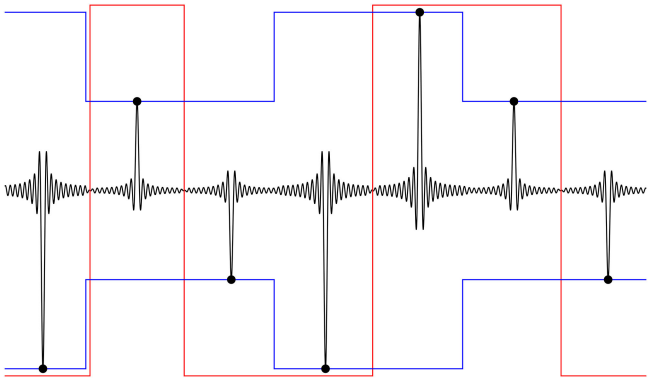

DOI: 10.1109/JPHOT.2019.2902726
1943-0655

IEEE photonics SOCIETY

IEEE

Orthogonal Full-Field Optical Sampling

Janosch Meier, Arijit Misra, Stefan Preußler, and Thomas Schneider

Institut für Hochfrequenztechnik, Technische Universität Braunschweig, 38106 Braunschweig, Germany

DOI:10.1109/JPHOT.2019.2902726

Manuscript received January 15, 2019; revised February 24, 2019; accepted February 27, 2019. Date of publication March 4, 2019; date of current version March 18, 2019. Corresponding author: Janosch Meier (e-mail: janosch.meier@ihf.tu-bs.de).

Abstract: Sampling is the first step to convert analogue into digital signals and one of the basic concepts for information handling. All practical sampling systems, however, are accompanied with errors. Bandwidth-limited signals can be seen as a superposition of time-shifted sinc pulses, weighted with the sampling values. Thus, due to orthogonality, bandlimited signals can be perfectly sampled by a corresponding sinc pulse with the correct time shift. But, sinc pulses are just a mathematical construct. Sinc pulse sequences, instead, can simply be generated by a rectangular, phase-locked frequency comb. For a high repetition-time to pulsewidth ratio, or a low duty cycle, the pulses of such a sequence come close to single sinc pulses, and thus, the sampling with them might lead to an almost ideal sampling. Here, we present the full-field optical sampling with a repetition-time to pulsewidth ratio of up to 153, or a duty cycle of around 0.65%. Since it enables amplitude and phase sampling, ultrahigh sampling rates should be possible.

Index Terms: Ideal sampling, optical sampling, optoelectronics.

1. Introduction

Today, almost all communication channels, storage devices and processing systems are digital. Thus, to transmit, store or change an analogue signal, it has to be sampled first. Additionally, in a high-bandwidth receiver even the transmitted and distorted digital data are sampled before they are further processed with electronics. Furthermore, most of today's measurement devices are digital as well, i.e., not the value itself but, its sampled version will be measured. Since ideal sampling is not possible in nature, these sampling devices have an error. Up to a certain extend this error might be compensated with an electronic post processing. However, with increasing data rates and bandwidths of the signals to be sampled, this becomes more and more complicated.

Mathematically, error-free, ideal sampling is a process, which accurately extracts the values of the bandwidth-limited signal to sample with an exact repetition rate instantaneously. This can be realized via the multiplication of the signal with a jitter-free ideal Dirac delta sequence. Since such a Dirac delta sequence is physically and practically not realizable, other methods have to be used [1], [2].

Electrical analogue-to-digital converters are typically based on sample and hold circuits. Due to the tremendous progress in CMOS and SiGe technology in the last few years, data converters with sampling rates of tens of GSa/s are available. Recently, an ADC with 72 GSa/s and 36 GHz input

bandwidth in 14 nm CMOS technology has been shown [3] for instance. Since electronic ADC can sample the whole field of the signal (amplitude and phase), much higher input bandwidths are possible by spectral interleaving [4]. But, at high bandwidths the accuracy of the sampling is typically limited by the phase noise or jitter of the clock, i.e., the inability to sample with a precise repetition rate. The best electronic ADC exhibit jitter levels of 50–80 fs, corresponding to the jitter of ultra-low phase noise quartz oscillators [5]. For high bandwidths and spectral interleaving this sampling error results in a decreasing resolution. In contrast, optical clocks like a mode-locked laser (MLL) can show very low jitter values in the attosecond range [6], [7]. However, to multiply the pulse sequence, generated by the MLL, with the signal, a nonlinear device like a crystal, a nonlinear effect in a fiber or a Mach-Zehnder modulator (MZM) is required [6], [8]. These nonlinearities might lead to additional distortions of the signal.

Additionally, the multiplication of the signal with a Dirac delta sequence in the time domain corresponds to a convolution of the signal spectrum with a frequency comb. Thus, for ideal sampling an unlimited number of exact equal copies of its spectrum are present in the frequency domain. For conventional electrical or optical sampling, instead, the shape of the envelope over all spectral copies is defined by the Fourier transform of the gating function in time domain used for the sampling. Due to the restricted rise and fall time, for electrical sampling the sample-and-hold functionality can be approximated by a trapezoidal function. However if, for the sake of simplicity, it is assumed as a rectangular function, it results in a sinc function in the frequency domain. For optical sampling with short pulses, these pulses can be approximated by a Gaussian function, leading to a multiplication of the spectra with a Gaussian shaped function as well. The electronic post-processing used for the compensation of this error becomes more and more complicated for increasing data rates and bandwidths.

Theoretically, instead of Dirac delta sequences, the multiplication of the signal with a corresponding sinc pulse with the right time shift and width leads to a perfect sampling as well. For the multiplication, again a nonlinear device like an intensity modulator can be used. This can be done either by the multiplication of the optical signal to sample with electrical Nyquist pulses, applied to the modulator [9], or the multiplication between optical Nyquist pulses with the electrical signal to sample. Optical Nyquist pulses can be achieved by spectral shaping of a MLL [10], or by a so called “Nyquist” laser [11]. However, these Nyquist pulses are not sinc-shaped, again a nonlinearity is required for the multiplication between signal and Nyquist pulse and the sampling and repetition rate is limited by the speed of the electronics and/or the bandwidth of the modulator.

A method for the generation of Nyquist pulses with a very high quality sinc shape was utilized for optical sampling by a convolution method [12]–[16]. Since this convolution works in the linear regime of the used intensity modulator, the distortions due to the nonlinearity are very low. However, the repetition-time to pulse-width ratio was only nine and therefore, far away from ideal single sinc pulses and only amplitude sampling has been shown so far. Thus, the sampling rate of this method is restricted by the bandwidth of the incorporated modulators.

Here we present a full-field (amplitude and phase) sampling with a sampling rate for periodical signals of 76.5 GSa/s with pulses with repetition-time to pulse-width ratios of up to 153 and discuss the potential of these low duty cycle pulses for almost ideal sampling, required for metrological applications for instance. The sampling rate of the method is only restricted by the bandwidth of the generated comb. By a parallelization in frequency or time domain, the real time sampling rate can correspond to the bandwidth of the pulses as well [13]. Since used in its linear regime, the sampling does not suffer from the nonlinear transfer function of the modulator. With a single modulator a sampling rate corresponding to three times – and with two coupled modulators, four times – the bandwidth of the modulator can be achieved [12]. Since the information of the full-field can be sampled, it has the potential to achieve ultrahigh sampling rates and bandwidths by spectrum interleaving for instance [4]. An integration on a silicon photonics platform might be straightforward and all sampling parameters like sampling rate, sampling time, bandwidth and so on can be precisely adapted to the optical signal to sample in the electrical domain.

2. Sampling Theory

Bandwidth-limited signals $A(t)$ can be written as the superposition of time shifted sinc pulses, weighted with the amplitude sampling values $a(\frac{k}{\Delta f_s})$ as:

$$A\,(t) = \sum_{k=-\infty}^{\infty} a\left(\frac{k}{\Delta f_s}\right) \mathrm{sinc}\,(\Delta f_s t - k). \tag{1}$$

Here, the sampling frequency Δf_s is more than twice the maximum baseband frequency of the signal and sinc is defined as:

$$\begin{aligned} \mathrm{sinc}\,(t) &= \left(\frac{\sin(\pi t)}{\pi t}\right) \textit{ for } t \neq 0 \\ \mathrm{sinc}\,(t) &= 1 \textit{ for } t = 0. \end{aligned} \tag{2}$$

If this signal is transferred to the optical carrier frequency f_c, it will become:

$$S(t) = A\,(t)\, e^{j(2\pi f_c t + \varphi(t))} \tag{3}$$

The sampling is carried out with a low bandwidth measurement device. Thus it can be assumed, th the measurement will not follow the optical frequency, which is typically in the range of around 193 THz (the C-band of oical telecommunications at 1550 nm). The optical phase $\varphi(t)$ can be seen as the phase of the optical signal at the time when the amplitude sampling value $a(\frac{k}{\Delta f_s})$ is taken. Thus, it can be assumed as $\varphi(\frac{k}{\Delta f_s})$ and due to the orthogonality between the sinc functions, it can be shown that

$$\int_{-\infty}^{\infty} a\left(\frac{k}{\Delta f_s}\right) e^{j\varphi\left(\frac{k}{\Delta f_s}\right)} \mathrm{sinc}\,(\Delta f_s t - k) \times \mathrm{sinc}\,(\Delta f_s t - k)\,\mathrm{d}t = \frac{1}{\Delta f_s} a\left(\frac{k}{\Delta f_s}\right) e^{j\varphi\left(\frac{k}{\Delta f_s}\right)} \tag{4}$$

and

$$\int_{-\infty}^{\infty} a\left(\frac{k}{\Delta f_s}\right) e^{j\varphi\left(\frac{k}{\Delta f_s}\right)} \mathrm{sinc}\,(\Delta f_s t - k) \times \mathrm{sinc}\,(\Delta f_s t - l)\,\mathrm{d}t = 0 \tag{5}$$

with $k, l \in I$, $k \neq l$, and I as the set of integer numbers. Thus, by a multiplication of the signal with a sinc pulse at distinct time and a following integration, the exact amplitude values can be extracted with:

$$\int_{-\infty}^{\infty} \sum_{k=-\infty}^{\infty} a\left(\frac{k}{\Delta f_s}\right) e^{j\varphi\left(\frac{k}{\Delta f_s}\right)} \mathrm{sinc}\,(\Delta f_s t - k) \times \mathrm{sinc}\,(\Delta f_s t - l)\,\mathrm{d}t = \frac{1}{\Delta f_s} a\left(\frac{l}{\Delta f_s}\right) e^{j\varphi\left(\frac{k}{\Delta f_s}\right)}. \tag{6}$$

$1/\Delta f_s$ is a constant, irrelevant for the concept. For the sake of simplicity, we have assumed that the ase of the second sinc function, used to multiply with the signal to sample, is zero. Thus, the convolution of the signal in the intensity modulators has no influence to the phase of the optical signal. In practice, a balanced receiver together with a local oscillator will be used to detect the phase. Thus, not the absolute phase of the signal but the relative phase in respect to that of the local oscillator will be sampled.

However, Equation (6) only holds for ideal unlimited sinc pulses, which are just a mathematical construct and, like the Dirac delta sequences, cannot be produced in practice. Additionally, for the multiplication in the optical domain a nonlinear device would be required. Instead, here for the sampling the convolution between a rectangular frequency comb with a large number of lines and the signal to be sampled in one or two coupled intensity modulators is exploited. A basic sketch of the concept is depicted in Fig. 1.

For a comparison, Fig. 1(a) shows ideal sampling in the frequency domain. The multiplication between the Dirac delta sequence and the signal in the time domain leads to a convolution between an unlimited frequency comb and the signal spectrum. For the bandwidth-limited signal, this corresponds to an unlimited number of equal copies of its signal spectrum, as shown in Fig. 1(a).

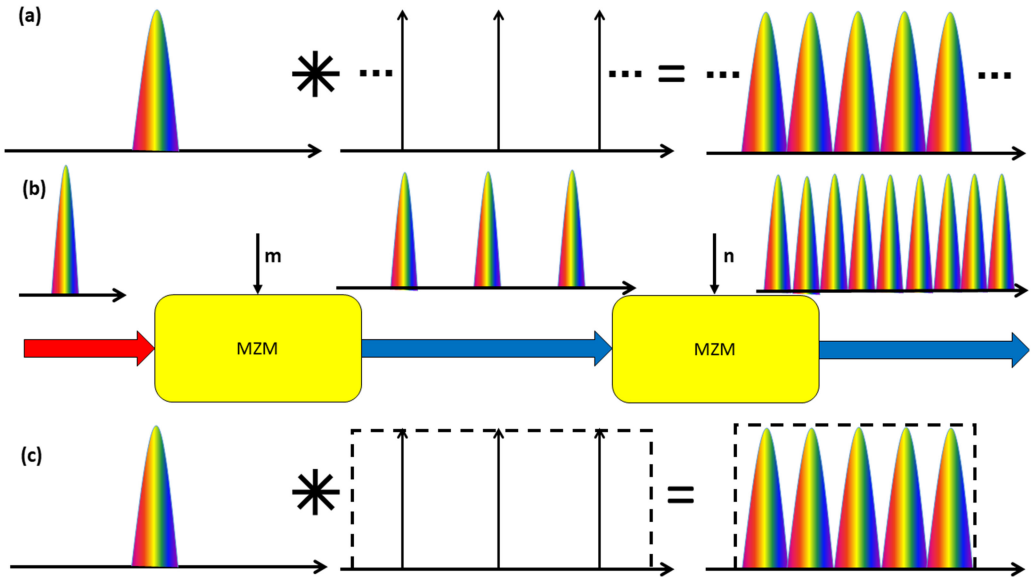

Fig. 1. Comparison between ideal and orthogonal sampling. For ideal sampling in the frequency domain (a) the signal spectrum is convoluted with an unlimited frequency comb resulting in an unlimited number of spectral copies. For the orthogonal sampling (b) the first Mach-Zehnder modulator (MZM) is driven with m RF frequencies, resulting in $2m + 1$ copies of the signal spectrum (here $m = 1$ and the number of copies is three). The second MZM, driven with n frequencies enhances this number to $(2m + 1)(2n + 1)$. Since here $m = n = 1$, the number of copies after the second MZM is nine. In the frequency domain (c) this corresponds to a convolution between the signal spectrum and a rectangular frequency comb with $C = (2m + 1)(2n + 1)$ lines. The only difference to ideal sampling (a) is that the number of equal copies is restricted by C.

For the convolution based sampling, an intensity modulator (here a Mach-Zehnder modulator, MZM) is driven with m sinusoidal frequencies (see Fig. 1(b)). By adjusting the bias voltage and RF power [12]–[16], at the output of the first MZM the spectrum in the middle and the copies with higher and lower center frequencies can have the same amplitude and are locked in phase. Since the input is a time-variant, bandwidth-limited signal, $2m + 1$ copies of the input spectrum are present at the output of the first MZM. The second modulator is driven with n sinusoidal frequencies and it is again adjusted in a way, that all newly generated copies have the same amplitude as the original ones. Thus, at the output the number of equal copies with locked phase is enhanced to $C = (2m + 1)(2n + 1)$. This convolution based sampling is shown in Fig. 1(c). It can be seen as a convolution of the input spectrum with a rectangular frequency comb. Thus, at the output a number of C equal copies with an equal or linear dependent phase are present.

The only difference between ideal (Fig. 1(a)) and convolution based sampling (Fig. 1(c)) is, that for convolution based sampling the number of equal copies is restricted to C. According to the discussion above, the higher the number C, the higher is the ratio between pulse-period and pulse-width and the closer the method comes to ideal sampling. Already with a few RF input lines m and n, a very high number of copies C can be achieved. A third modulator can enhance this number further. Following Equation (5), the single sampling points can be extracted by an integration over isolated pulses of the sinc sequence with a low bandwidth photodiode. The integration range is limited by the periodicity of the sinc sequence. For a sampling of amplitude and phase, a low bandwidth balanced receiver and a local oscillator are required. The higher the pulse-period to pulse-width ratio, the lower are the requirements to the bandwidth of the detector.

If the optical input spectrum to the one or two coupled modulators consists of just one continuous wave (cw) line, the output of the sampling device is a number of C equidistant copies of this line, or a rectangular frequency comb with C lines. In the time domain, this corresponds to a sinc pulse

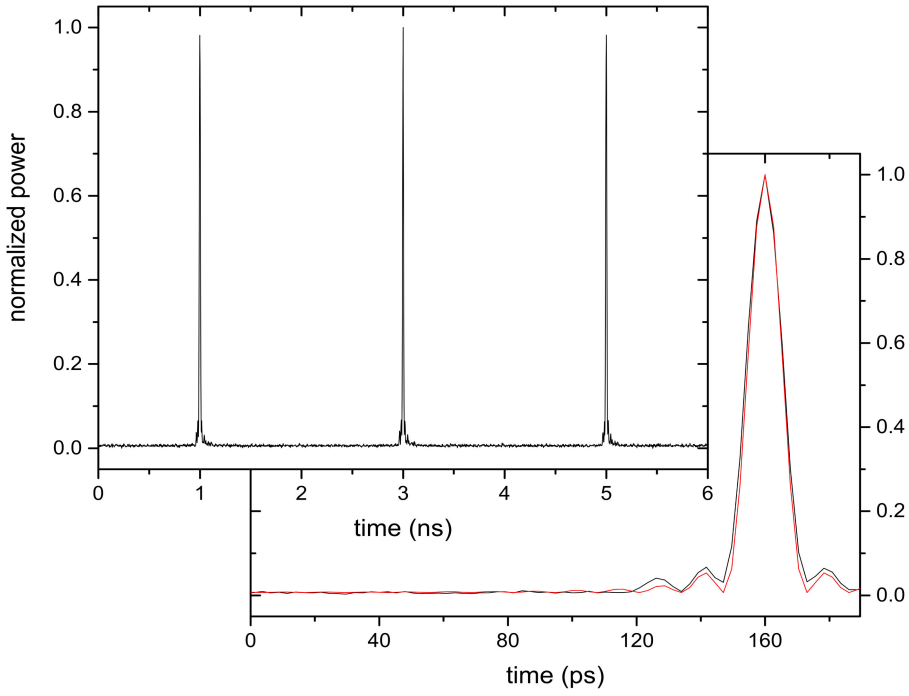

Fig. 2. Sinc pulse sequence generation for an optical cw input line. Experimental results (black) and simulation (red) for a sinc pulse sequence generated by two coupled modulators driven with $m = 25$ and $n = 1$ input frequencies. The data are shown with different time scales. 153 copies of a cw input wave with a spacing of 500 MHz are generated, leading to sinc pulses with a full-width at half-maximum duration of around 13 ps, or a duty cycle of around 0.65%.

sequence, which is the unlimited superposition of single time-shifted sinc pulses [12]:

$$\left(\frac{\sin(\pi C \Delta f t)}{C \sin(\pi \Delta f t)}\right) = \sum_{k=-\infty}^{\infty} \operatorname{sinc}(C(\Delta f t - k)) \quad \text{for} \quad \Delta f t \notin I$$

$$\left(\frac{\sin(\pi C \Delta f t)}{C \sin(\pi \Delta f t)}\right) = 1 \quad \text{for} \quad \Delta f t \in I \tag{7}$$

For an optical cw input line with a frequency spacing of 500 MHz Fig. 2 presents the measured and simulated pulses for a rectangular frequency comb with 153 lines ($m = 25$, $n = 1$).

3. Experimental Results

The experimental setup is depicted in Fig. 3. The first modulator was driven with $m = 25$ radio frequencies with a frequency spacing of 500 MHz. By the bias voltage at the modulator and the RF power, the modulator was adjusted in a way that the 25 lower and upper frequency lines, or spectral copies of the input signal, have the same power as the carrier [12], [15], resulting in 51 copies of the input spectrum with an overall bandwidth of $51 \times 500\,\text{MHz} = 25.5\,\text{GHz}$. The second modulator is driven with just one radio frequency of 25.5 GHz, generated by an RF generator. Since the 25 frequencies driving the first and the single frequency driving the second modulator have to have the same or a linear dependent phase, the AWG and the RF generator have to be synchronized to each other, as depicted in Fig. 3. The environmental conditions are stabilized over a specific time, in which all measurements were carried out. An automatic adjustment and compensation of the bias voltage drift would be possible with a feedback loop [13].

With $m = 25$ and $n = 1$, the number of generated copies behind the two modulators is 153. In the corresponding time domain this gives a multiplication of the input time signal with a sinc pulse

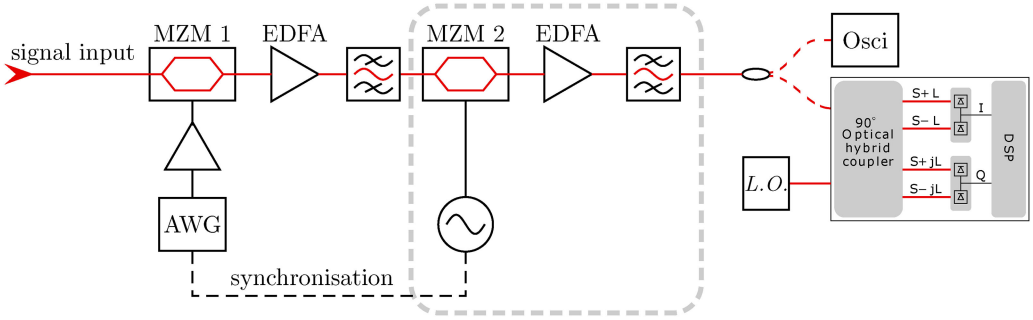

Fig. 3. Experimental setup. The first modulator was driven with $m = 25$ sinusoidal frequencies generated by an arbitrary waveform generator (AWG). To triple the number of generated copies, the second modulator was driven with $n = 1$ frequency, generated by an RF generator, synchronized with the AWG. Since for the benefit of a lower setup complexity the second modulator could be omitted, this part is shown in a grey dashed box. For the amplitude sampling, the optical input signal was a sinusoidal wave generated by another intensity modulator (not shown). For the amplitude and phase sampling, the optical input signal was a sinusoidal and phase modulated wave generated by an intensity and phase modulator (as well not shown). For the detection of the amplitude modulated signal an electrical oscilloscope with a bandwidth of 70 GHz, and for the detection of the amplitude and phase sampling a balanced detector with a bandwidth of 33 GHz has been used. EDFA: erbium-doped fiber amplifier, Osci: oscilloscope, L.O.: local oscillator, DSP: digital signal processor.

sequence with a pulse width (from the maximum to the first zero crossing) of $\tau_p = 1/(3(2m+1)\Delta f) \approx 13\,\text{ps}$ and 152 zero crossings between two consecutive pulses. Thus, the repetition-time to pulse-width ratio is 153 and the duty cycle is around 6.5×10^{-3} or 0.65%.

The signal to sample was generated by a cw laser externally modulated by an MZM. By a phase shift of the electrical signal, the sinc pulse sequence is shifted through the signal to sample. This requires synchronization between the signal to sample and the sampling block. In a measurement device this can be realized by a clock recovery.

The bandwidth of the sampling pulses was with $153 \times 0.5\ \text{GHz} = 76.5\,\text{GHz}$ above the bandwidth of our electrical measurement equipment. For the measurement an electrical sampling scope has been used. With a nonlinear measuring head, the bandwidth of this scope was increased to 70 GHz. Thus, the black squares in Fig. 4 show the integration value over the sampling pulses achieved with the lower bandwidth electronic equipment. The colored traces depict the ideally expected sinc pulses, with the right bandwidth and time shift. As can be seen, the sampling pulses follow the signal to sample very well which indicates a high sampling quality. We address the slight differences between the waveform and the sampling points to imperfections of our proof of concept setup. The same holds for jitter and noise. For the sake of simplicity, the 25 radio frequencies for the first generator were generated by an arbitrary waveform generator (AWG). The AWG had a phase noise of around -130 dBc/Hz at an offset of 10 kHz for a frequency of 500 MHz and the jitter value is around 250 fs. With laboratory-grade RF generators in the same setup, jitter values of below 100 fs can be achieved [12]. Additionally, the AWG can be replaced by extremely high-quality RF sources, which can reach jitter values in the zeptosecond range [17] and phase noise values down to -167 dBc/Hz at an offset of 10 kHz [18]. In combination with frequency multipliers or mixers, as well as integrated CMOS chips, such high-quality RF sources directly can generate electrical phase-aligned multitone waveforms. Since each phase change of the electrical and optical signal leads to a time shift of the sampling points, we assume that only an integrated solution will result in very high quality sampling. Since only one or two coupled modulators are required for the setup, such an integration might be straightforward but is not available at the moment. Due to the successive executed measurements, the sampling rate for a periodical signal coincides to the bandwidth of the comb and is 76.5 GSa/s. However, the real time sampling rate is given by the pulse repetition rate, or the the spacing of the comb lines to be 500 MSa/s. By a splitting of the signal to sample into several measurement channels and a parallelization in time, the real time sampling rate can as well

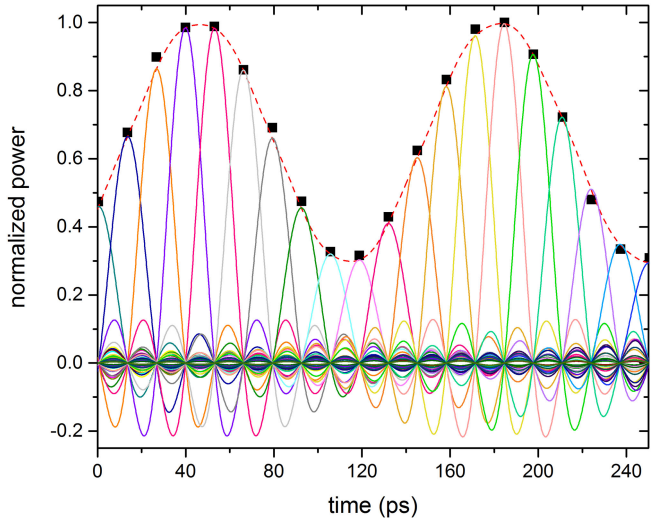

Fig. 4. Amplitude sampling with a repetition-time to pulse-width ratio of 153. Sampling of a 7.65 GHz sinusoidal signal by generating 153 equal copies of the signal spectrum, or by the multiplication of the signal with a sinc pulse sequence with a repetition-time to pulse-width ratio of 153, corresponding to a duty cycle of 0.65%. The black squares show the integration of the sampling values over the repetition rate. Because of the restricted storage capacity of the oscilloscope, the integration was carried out in the range of ± 250 ps from the pulse center. Since the bandwidth of the single pulses is above that of our measurement equipment, the colored lines show the simulated ideal sampling pulses that build the sine wave by summation.

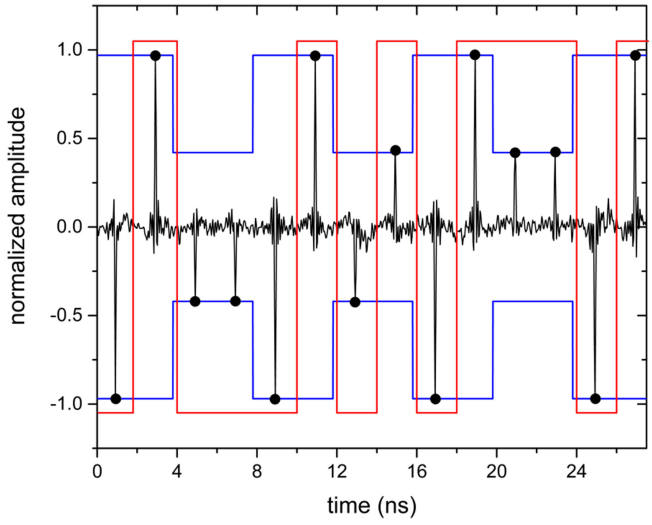

Fig. 5. Amplitude and phase sampling. A square wave signal with two phase states is sampled by generating 153 equal copies of the signal spectrum, or by the multiplication of the signal with a sinc pulse sequence with a duty cycle of around 0.65%. The signal to sample is intensity modulated with a 250 MHz rectangular wave (blue trace). Additionally the signal is phase modulated by a PRBS 9 signal with a binary phase shift keying and a symbol rate of 500 Mbd (red).

be enhanced up to the comb bandwidth. A detailed discussion about parallelization and examples for the sampling of arbitrary signals can be found in [13].

To have a known phase for the phase measurements, the amplitude modulated signal to sample was additionally modulated by a phase modulator (PM). The detection was carried out with a coherent detector consisting of a balanced receiver, a local oscillator and an electrical sampling scope

with an analogue bandwidth of 33 GHz. Frequency differences between the local oscillator and the signal source are compensated by a digital signal processor and a following signal processing software in the sampling scope.

The amplitude and phase sampling with a repetition-rate to pulse-width ratio of 153 is shown in Fig. 5. A square wave with a repetition rate of 125 MHz is additionally phase modulated with a PRBS signal with a symbol rate of 500 Mbd. Here again the bandwidth of the sampling pulses was almost 80 GHz and therefore much higher than the electrical bandwidth of the balanced detector (33 GHz). However, as depicted in Fig. 4, the integration over the distorted pulses gives the correct amplitude and phase values.

4. Conclusion

In conclusion, a full-field sampling method (amplitude and phase), which exploits the orthogonality of sinc pulses, has been introduced. In proof-of-concept experiments, amplitude and phase sampling with a rate of up to 76.5 GSa/s for periodical signals and repetition-time to pulse-width ratios of up to 153, or a duty cycle of 0.65% has been shown. Since for low duty cycles the method comes close to ideal sampling, it might be very advantageous for metrology and other applications requiring a precise sampling. All sampling parameters like sampling rate, sampling time and so on can directly be adjusted in the electrical domain. Thus, the sampling can be easily and precisely adapted to the signal to sample. By only one MZM a maximum sampling rate of 3 times the bandwidth of the electrical components and the MZM is possible [12]. The number of generated copies of the input spectrum corresponds to $2m + 1$, with m as the number of input frequencies. By the incorporation of a second coupled intensity modulator, the sampling rate can be increased to 4 times the bandwidth of the modulator with the highest bandwidth [12], [13]. The number of generated copies will be increased to $(2m + 1)(2n + 1)$ with m and n as the number of radio frequencies driving the first and the second modulator. With integrated modulators with a bandwidth of 100 GHz [19], [20] sampling rates of 400 GSa/s would be possible. However, since the method enables a low error and full-field sampling, even low bandwidth modulators could reach much higher sampling rates in the TSa/s range with spectrum interleaving methods [4]. Additionally, it requires no mode-locked nor other laser sources, it can be integrated on a CMOS compatible platform and it might overcome the analogue bandwidth restrictions from pure electrical sampling, avoiding the complexity of high bandwidth optical pulse sampling.

References

[1] R. van de Plassche, *CMOS Integrated Analog-to-Digital and Digital-to-Analog Converters*. New York, NY, USA: Springer-Verlag, 2013.

[2] Y.-R. Sun and S. Signell, "Effects of noise and jitter on algorithms for bandpass sampling in radio receivers," in *Proc. IEEE Int. Symp. Circuits Syst.*, Vancouver, BC, Canada, 2004, pp. 761–764.

[3] L. Kull *et al.*, "A 24-to-72GS/s 8b time interleaved SAR ADC with 2.0-to-3.3pJ/conversion and >30dB SNDR at nyquist in 14nm CMOS FinFET," in *Proc. IEEE Int. Solid-State Circuits Conf.*, San Francisco, CA, USA, 2018, pp. 358–360.

[4] N. K. Fontaine, R. P. Scott, L. Zhou, F. M. Soares, J. P. Heritage, and S. J. B. Yoo, "Real-time full-field arbitrary optical waveform measurement," *Nature Photon.*, vol. 4, pp. 248–254, 2010.

[5] *Ultra Low Phase Noise Oven-Controlled Crystal Oscillator OX-305 at 100 MHz*, Vectron Int., Hudson, NH, USA, 2016.

[6] A. Khilo *et al.*, "Photonic ADC: Overcoming the bottleneck of electronic jitter," *Opt. Exp.*, vol. 20, no. 4, pp. 4454–4469, Feb. 2012.

[7] A. H. Nejadmalayeri *et al.*, "Attosecond photonics for optical communications," in *Proc. Opt. Fiber Commun. Conf. Expo./Nat. Fiber Opt. Eng. Conf.*, Los Angeles, CA, USA, 2012, pp. 1–3.

[8] R. Salem, A. Foster, A. C. Turner-Foster, D. F. Geraghty, M. Lipson, and A. L. Gaeta, "High-speed optical sampling using a silicon-chip temporal magnifier," *Opt. Exp.*, vol. 17, no. 6, pp. 4324–4329, Mar. 2009.

[9] V. Vercesi, D. Onori, J. Davies, A. Seeds, and C.-P. Liu, "Electronically synthesized Nyquist pulses for photonic sampling of microwave signals" *Opt. Exp.*, vol. 25, no. 23, pp. 29249–29259, Nov. 2017.

[10] M. Nakazawa, H. Toshihiko, R. Peng, and G. Pengyu, "Ultrahigh-speed "orthogonal" TDM transmission with an optical Nyquist pulse train," *Opt. Exp.*, vol. 20, no. 2, pp. 1129–1139, Jan. 2012.

[11] M. Nakazawa, M. Yoshida, and T. Hirooka, "The Nyquist laser," *Optica*, vol. 1, no. 1, pp. 15–22, Jul. 2014.

[12] M. A. Soto *et al.*, "Optical sinc-shaped Nyquist pulses of exceptional quality," *Nature Commun.*, vol. 4, pp. 1–11, Dec. 2013.

[13] S. Preußler, G. R. Mehrpoor, and T. Schneider, "Frequency-time coherence for all-optical sampling without optical pulse source," *Sci. Rep.*, vol. 6, pp. 1–10, Sep. 2016.
[14] S. Preußler, N. Wenzel, and T. Schneider, "Flexible nyquist pulse sequence generation with variable bandwidth and repetition rate," *IEEE Photon. J.*, vol. 6, no. 4, pp. 1–8, Aug. 2014.
[15] S. Preußler, N. Wenzel, and T. Schneider, "Flat, rectangular frequency comb generation with tunable bandwidth and frequency spacing," *Opt. Lett.*, vol. 39, no. 6, pp. 1637–1640, 2014.
[16] M. A. Soto *et al.*, "Generation of Nyquist sinc pulses using intensity modulators," in *Proc. CLEO: Sci. Innov.*, San Jose, CA, USA, 2013, pp. 1–2.
[17] X. Xie *et al.*, "Photonic microwave signals with zeptosecond-level absolute timing noise," *Nature Photon.*, vol. 11, pp. 44–47, Nov. 2016.
[18] X. Xie *et al.*, "Record ultra-low phase noise 12 GHz signal generation with a fiber optical frequency comb and measurement," in *Proc. CLEO: OSA Tech. Dig.*, San Jose, CA, USA, 2016, pp. 1–2.
[19] L. Alloatti *et al.*, "100 GHz silicon-organic hybrid modulator," *Light Sci. Appl.*, vol. 3, pp. 1–4, May 2014.
[20] C. Wang *et al.*, "Integrated lithium niobate electro-optic modulators operating at CMOS-compatible voltages," *Nature*, vol. 562, pp. 101–104, Sep. 2018, doi: 10.1038/s41586-018-0551-y.